IJFANS INTERNATIONAL JOURNAL OF FOOD AND NUTRITIONAL SCIENCES
ISSN PRINT 2319 1775 Online 2320 7876
 Journal Volume 11 S Iss 01, 2022

Batch sorption studied of reduced graphene oxide /calcium alginate beads for efficient removal of fluoride and chromium from water

Darshana A. Fendarkar
Department of Chemistry, Govt. Institute of Science, R.T. Road, Civil Lines,
Nagpur – 440001 (MS) India.

Abstract:
Reduced graphene oxide /calcium alginate beads (rGO/calcium alginate beads) were composed of reduced graphene oxide and calcium alginate which was prepared by sol-gel method and characterized by SEM, TEM, XRD and IR. To study the effect of various factors like adsorbent dose, initial concentration, pH and temperature on fluoride and chromium removal from water using rGO/calcium alginate beads a series of batch sorption experiments were conducted. The obtained results were analyzed by Langmuir and Freundlich isotherms and it was found that fluoride and chromium removal closely follows Langmuir adsorption isotherm. The results were also analyzed through various kinetic models like Lagergreen pseudo-first-order kinetics, the pseudo-second-order kinetics, and the intraparticle diffusion model. Removal of fluoride and chromium from water is best described by the pseudo-second-order Lagergreen equation. It was also found that intra-particle transport is not the rate-limiting step.

Keywords: reduced graphene oxide, calcium alginate, kinetics, adsorption isotherm, fluoride removal, chromium removal.

1. Introduction:

With the fast development of industry, wastewater from various industries such as metal finishing, electroplating, plastics, and mining, containing several harmful ions of health and environmental concern such as mercury [1], cadmium, copper, chromium, zinc, nickel [2], fluoride [3], arsenic [4], and other ions, have been discharged in an environment with an increasing amount. Widespread occurrence of fluoride in groundwater more than the prescribed limit has caused multidimensional health problems [5, 6]. Various methods have been used to remove fluoride from water, including adsorption [7, 8], precipitation [9, 10], ion exchange [11], Donnan dialysis [12], electrodialysis [13], reverse osmosis [14], and nanofiltration [15]. Among them, adsorption is recognized as the most convenient, effective, and economical method of drinking water purification [16, 17]. Numerous adsorbents have been studied for the removal of fluoride from water. Alumina-based adsorbents [18], metal oxides [19-21], clays [22, 23], carbons [24], zeolites [25], and even industrial/agricultural wastes [26] possess the ability to adsorb fluoride. However, low adsorption capacity restrains their applications. To achieve high adsorption capacity, some rare earth-containing adsorbents were studied for fluoride removal [27]. During past decades various scientists have worked on fluoride and chromium removal by using various adsorbents such as Singh et al. in 2013 utilized alginate nanoparticles prepared by nanoparticles of sodium alginate cross-linked ferric chloride for fluoride removal from water bodies, Langmuir adsorption was found to be 0.697 mg/g [28]. Sujana et al. (2013) utilized

hydrous ferric oxide doped alginate beads for fluoride removal from water the Langmuir adsorption capacity was 8.90 mg/g [29]. Prabhu et al. (2015) synthesized alginate-zirconium complex oxalic acid (Ox), malonic acid (MA) and succinic acid (SA). Complexes like alginate-oxalic acid-zirconium (Alg-Ox-Zr), alginate-malonic acid-zirconia (Alg-MA-Zr), as well as alginate-succinic acid-zirconium (Alg-SA-Zr), were made and utilized for fluoride removal from water. The maximum adsorption capacity of Alg-Ox-Zr, Alg-MA-Zr and Alg-SA-Zr complexes were found to be 9.653, 4.851 and 4.059 mg/g respectively [30]. Pandi and Viswanathan (2015) synthesized alginate beads filled with nano-hydroxyapatite and the resulting solution was cross-linked with La (III) (n-HapAlgLa) for fluoride removal of water. The Langmuir maximum adsorption capacity of the n-HapAlgLa bead was 4.536 mg/g [31].

In our study, we used graphene oxide calcium alginate beads for fluoride and chromium removal. Because graphene oxide (GO) has a large specific surface area and high hydrophobicity. There could be a wide series of interactions between the intrinsic functional groups implanted on GO and contaminants. These properties make GO highly desirable for applications in water remediation. Alginate is a copolymer composed of α-D-annotate (M) and β-L-guluronate (G) units linked by β-1, 4 and α-1,4 glycosidic bonds, with M and G residues present in various proportions and sequences [9]. It is mainly extracted from brown algae or seaweeds [10]. It has attracted much attention on account of its biocompatible and biodegradable properties, and rapid gelation ability in many fields. Alginate gelation occurs when divalent cations (Ca^{2+}, Fe^{3+}, Al^{3+}, Zr^{4+}) interact with blocks of G residues, divalent ions diffuse into the sodium alginate solution and replace Na+ with a rapid, strong and irreversible formation of gel [11]. Because of high electronegativity and small ionic size, fluoride ion is classified as a hard base [12]. Therefore, it has a strong affinity towards electropositive multivalent metal ions like Fe^{3+}, Ca^{2+}, Zr^{4+}, La^{3+}, Ce^{4+}, and Al^{3+}. Solidification of positively charged cations onto the material helps to create positive charges which could be used to solidify F- [13]

2. Material and Method:

Graphite powder, H_2SO_4, $NaNO_3$, $KMnO_4$, H_2O_2, HCl, acetone, sodium alginate, calcium chloride and all other chemicals were purchased from Merck (AR) and used as it is without further purification.

Graphene oxide (GO) was synthesized according to the method reported by Hummers from purified natural graphite powder [14]. Then reduced graphene oxide (rGO) was prepared from graphene oxide by using sodium borohydride according to the method reported by K.M. Nalin de Silva et al. Graphene oxide dispersion (1mg/ml) was transferred to a 250 ml conical flask and 1g of sodium borohydride and some quantity of ammonium hydroxide solution was added to the graphene oxide dispersion and pH was adjusted to 10. Then the solution was stirred for a few minutes and was heated to 95°C for 1 hour. The prepared mixture was filtered through a filter paper and the precipitate was washed with double distilled water several times. For preparing rGO/calcium alginate beads, 5 gm of reduced GO (rGO) powder was mixed with 5 gm of sodium alginate in 100 ml distilled water and stirred for 24 hrs. After 24 hrs this mixture was filled into

the burette. 1 molar calcium chloride solution ($CaCl_2$) was prepared in a beaker and this beaker of $CaCl_2$ solution was kept below the burette which was filled previously. The flow of the burette was adjusted in such a way that only one bead was formed at a time. Then beads were washed several times with water and used for fluoride and chromium removal study. The fluoride and chromium removal study was carried out by the kinetic study. Fluoride and chromium solution of the following concentration was prepared which are as follows 10 ppm, 20 ppm, 30 ppm of fluoride solution and 6ppm, 8 ppm, and 10 ppm of chromium solution etc. Then 0.2 gm of rGO calcium alginate beads was taken in three different beakers and 100 ml of 10 ppm, 20 ppm, & 30 ppm fluoride solution was added into that beaker and stirred at room temperature. Simultaneous reaction was carried out at 40˚C and 60˚C temperature. Also, 0.2 gm of calcium alginate beads were added into the 6 ppm, 8 ppm and 10 ppm of chromium solution. The amount of fluoride and chromium removed per unit mass of the adsorbent was evaluated by using the following mass balance equation,

$$q = \frac{(Co-Ce)V}{W}$$

The percent removal of fluoride and chromium was calculated as follows:

$$\% \text{ Removal of fluoride/chromium} = \frac{C_{initial}-C_{Final}}{C_{initial}} \times 100$$

The effect of adsorbent dosage level on the per cent removal of fluoride and chromium was studied using fluoride concentrations of 10 ppm and 20 ppm and chromium concentrations of 6 ppm and 8 ppm solution. 0.2 gm to 0.8 gm calcium alginate beads were added into 10 ppm and 20ppm fluoride solution as well and the same amount of calcium alginate beads were added into 6ppm and 8ppm of chromium solution stirred all the solutions for some time then aluminium salt and aluminon dye were added into the same beaker and absorbance was taken on UV –Visible spectrophotometer at 516 nm for fluoride and 542 nm for chromium removal.

The samples were characterized by scanning electron microscopy (JEOL Model JSM - 6390LV field-emission). Transmission electron microscopy (TEM PHILIPS CM 200 at 20-200 kV resolutions). Fourier transforms infrared Spectroscopy (FT-IR Brucker), X-ray diffraction (XRD- SHIMADZU 500 XRD analyzer)

3. Results and Discussion:

The XRD pattern of rGO/calcium alginate beads was shown in Fig. 1 GO had a typical peak around 10.20˚ corresponding to interlayer space around 8.66 Å. The spectrum of sodium alginate(SA) shows the characteristic crystalline peaks at 2θ=12.25˚and 20.75˚ may be due to the lateral packing among molecular chains and the layer spacing along the molecular chain direction in sodium alginate [15], respectively. After the addition of graphene oxide, the rGO/calcium alginate beads show a small reduction in d-spacing value from 6.01 A˚ (SA) to 3.06 A˚(SA-GO) indicating a possible interaction between the carboxyl groups of sodium alginate with hydroxyl groups of GO [15].

ISSN PRINT 2319 1775 Online 2320 7876
 Journal Volume 11 S Iss 01, 2022

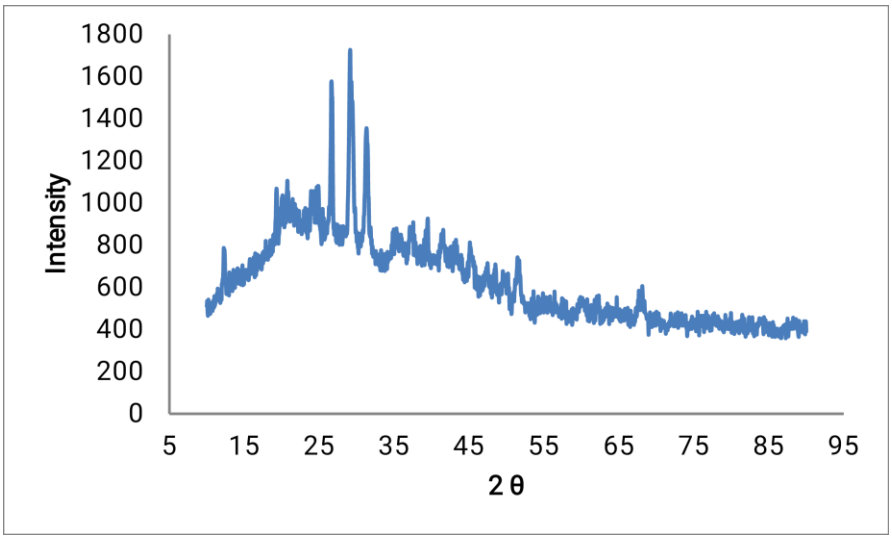

Fig 1 XRD Spectra of rGO/Calcium alginate beads

The morphological characteristic of rGO/calcium alginate beads was carried out by SEM analysis and corresponding results are shown in Fig.2, the dry rGO/calcium alginate are spherical with about 1.12 mm in diameter obviously, and the size of dry rGO/calcium alginate was much smaller than that of wet rGO/calcium alginate, which was about 3.41 mm. In addition, the surface microstructure of rGO/calcium alginate beads has a globular morphology with a highly rough surface.

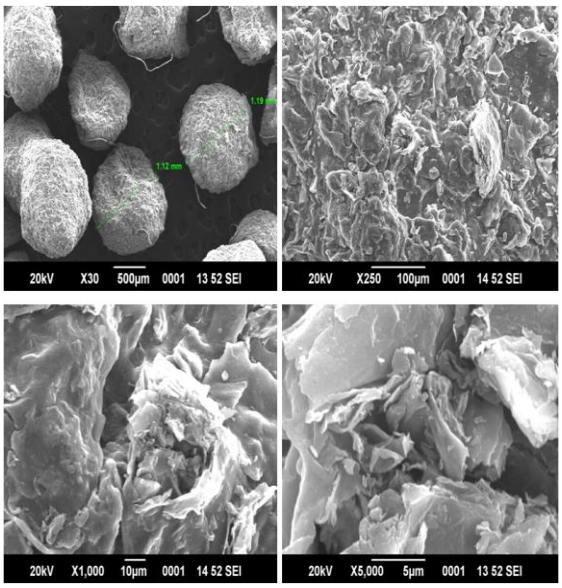

Fig. 2 SEM images of rGO/calcium alginate bead

TEM images of rGO/calcium alginate beads show that the calcium alginate is deposited on the rGO sheets in Fig. 3. Further it is observed that the calcium alginates were deposited on the fold (wrinkles) area of GO sheets where maximum functional groups are present. This confirms our earlier hypothesis which we drew in SEM observation.

ISSN PRINT 2319 1775 Online 2320 7876
 Journal Volume 11 S Iss 01, 2022

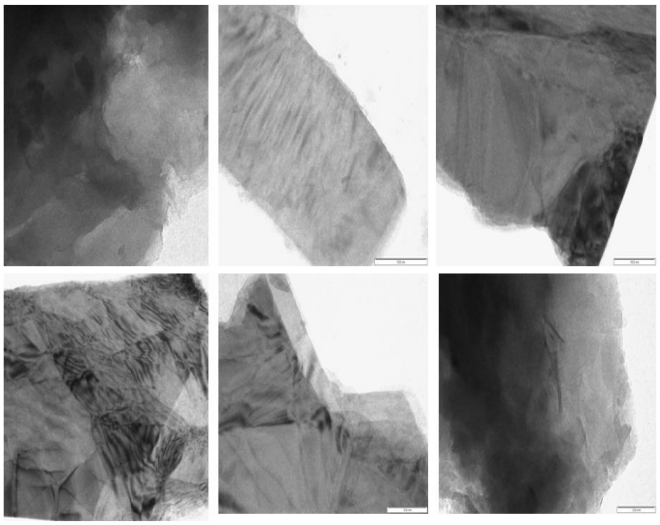

Fig. 3 TEM images of rGO/ Calcium alginate beads

FT-IR spectra were used to characterize the interaction between rGO and the polymer chains of the hydrogel. As shown in Fig. 4 the broad and intense peak of O–H groups centred at 3302.34 cm^{-1} indicates the interaction of GO with alginate, The peaks at 1415cm^{-1} and 1595cm^{-1} indicated the symmetric and asymmetric stretching vibrations of carboxylate, respectively, in some metal-alginate interactions [16]. In our GO/calcium alginate composite, the symmetric and asymmetric stretching vibrations of carboxylate ion were observed at 1593.96 cm^{-1} and 1412.74 cm^{-1}. This confirms the calcium alginate interaction in the GO/calcium alginate composite. Asymmetric stretching vibration of carboxylate ion shifted to lower wave numbers because when calcium metal ions replaced sodium ions in the sodium alginate, the charge density, the radius and the atomic weight of the cation were changed and hence, this shifting should be expected. This shift and presence of all the vibration of alginate shows the formation of rGO/calcium alginate beads. Now GO/calcium alginate binds with calcium and carries a positive charge which tends to adsorb a negatively charged fluoride ion and $Cr_2O_7^-$ ion.

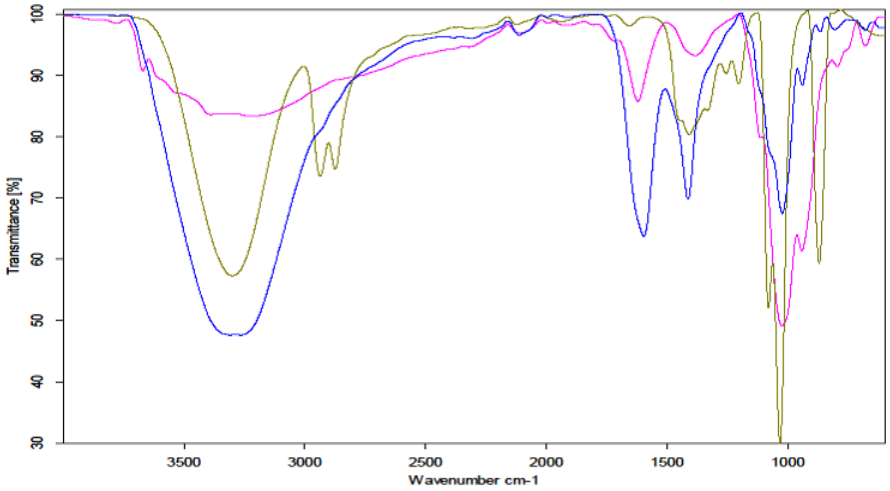

Fig. 4 FT-IR spectra of rGO (pink), rGO/calcium alginate (Blue) and Sodium alginate (green)

ISSN PRINT 2319 1775 Online 2320 7876
 Journal Volume 11 S Iss 01, 2022

Various adsorption parameters for the effective removal of fluoride and chromium using rGO/ calcium alginate beads as an adsorbent from an aqueous solution were studied and optimized. The effect of adsorbent dose on fluoride and chromium removal at fixed initial fluoride and chromium concentration is shown in Fig.5. It was observed that the percentage removal of fluoride as well as chromium increased with the increase in adsorbent dose. This can be explained by the fact that the greater the mass of the adsorbents, the larger the contact surface offered for the adsorption. Increases in rGO/calcium alginate compound concentration increase the level of adsorption of fluoride and Cr (VI) ions because of an overall increase in the surface of rGO-calcium alginate compound which in turn increases the no of binding sites leads to the increase of fluoride and chromium removal efficiency. Therefore more rGO/calcium alginate compound provides more active sites for impact with fluoride and Cr (VI) molecules to accelerate the fluoride and Cr (VI) removal efficiency.

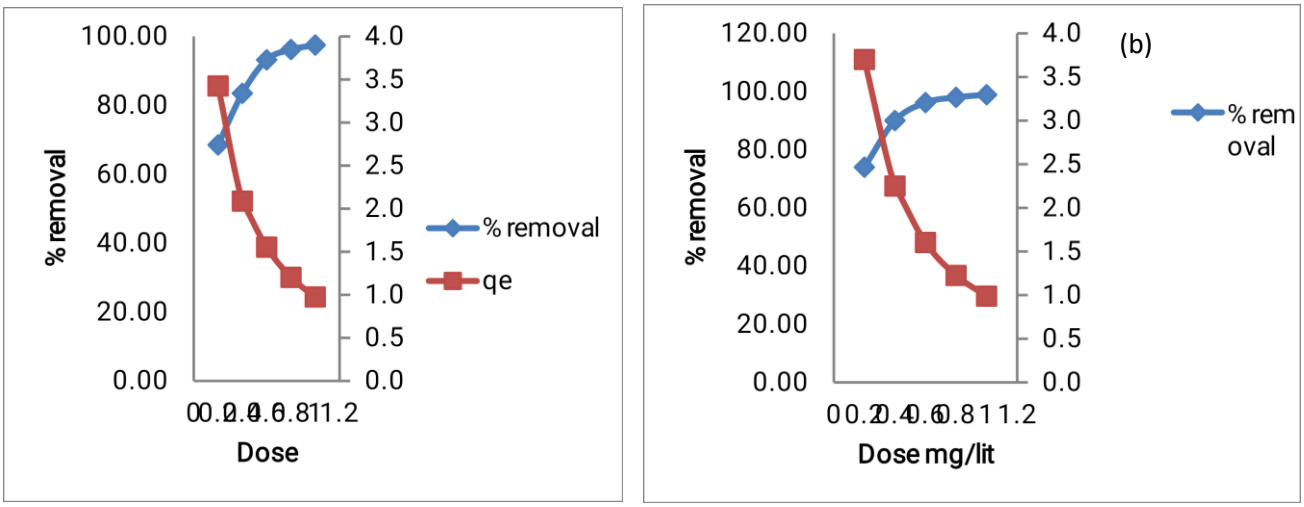

Fig. 5 Effect of adsorbent dose on the % removal of (a) fluoride and (b) chromium

The effect of initial concentration on the percentage removal of fluoride and chromium was studied at different initial fluoride and Cr (VI) concentrations by keeping other parameters constant. The effect of initial concentration on removal of fluoride and Cr (VI) is shown in Fig. 6. It was observed that with the increase in fluoride and chromium initial concentration, the percentage removal of fluoride and chromium decreases. This may be because at higher adsorbate concentration, the binding capacity of the adsorbent approaches saturation, resulting in a decrease in overall per cent removal.

ISSN PRINT 2319 1775 Online 2320 7876
 Journal Volume 11 S Iss 01, 2022

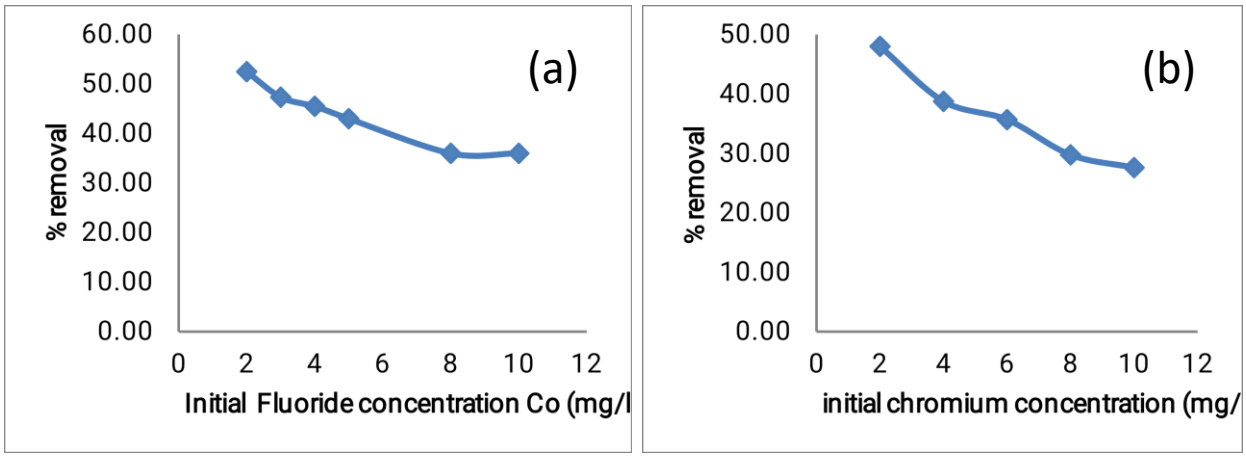

Fig. 6 Effect of initial concentration of (a) fluoride and (b) chromium on removal by rGO/calcium alginate beads.

The pH of a solution is an important parameter in the adsorption process. Fig.7 shows the effect of pH on the removal efficiency of fluoride and chromium by rGO/calcium alginate beads. During this study, results revealed that the removal of fluoride was strongly dependent on the pH of the solution. The effect of pH on the adsorption of fluoride onto rGO-calcium alginate beads was studied at pH 3.0–12.0, and the maximum removal capacity of rGO-calcium alginate beads was found to be at pH 8.61 Percentage of removal increased rapidly with the increase in pH of the solution initially, and the optimal pH was observed at pH 8.61 Further increase in pH causes a drastic decrease in the adsorption percentage. This might be due to the weakening of the electrostatic force of attraction between the oppositely charged adsorbate and adsorbent which ultimately leads to the reduction in sorption capacity. While that of chromium removal, the amount of Cr (VI) adsorbed by rGO-calcium alginate beads varied significantly with solution pH. The optimum pH for the adsorption of Cr (VI) by rGO-calcium alginate beads was found to be 5.61. The Cr (VI) removal rate depends significantly on the pH of the solution because the solubility of the precipitate is strongly reliant on pH. The pH value of the solution changed slightly during the reaction process. It is evident that the reduction rate of Cr (VI) was greatly reduced under alkaline conditions because at low pH =5.61 the dominant form of Cr (VI) is $HCrO_4^-$ species shift to another form CrO_4 and $Cr_2O_7^{2-}$the decrease in removal of chromium by increasing the pH is due to the competition between CrO_4^{2-} and OH^-.

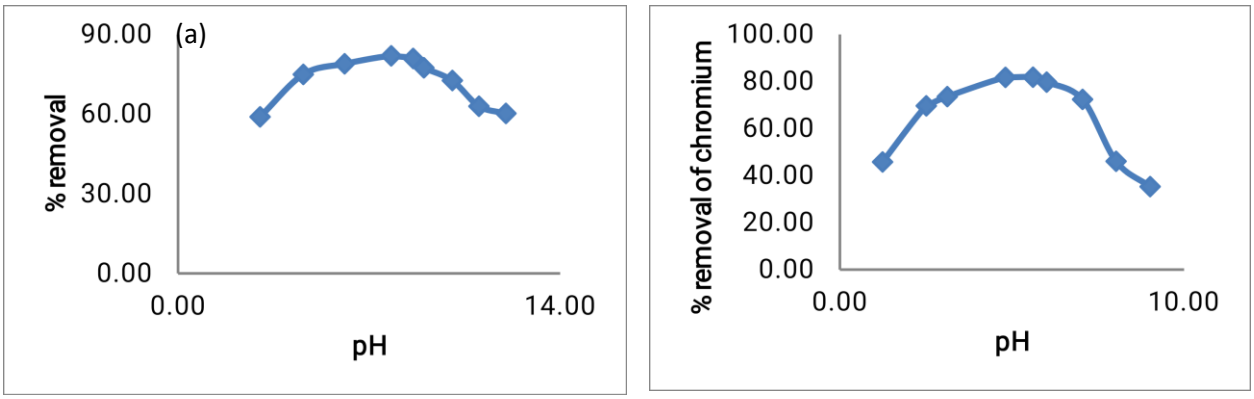

Fig. 7 Effect of pH on (a) fluoride and (b) chromium removal efficiency by using

ISSN PRINT 2319 1775 Online 2320 7876
 Journal Volume 11 S Iss 01, 2022

rGO/calcium alginate beads.

Langmuir and Freundlich's adsorption isotherm models are used to determine the mechanistic parameters associated with fluoride and chromium adsorption [17, 18]. The Langmuir-type isotherm shows relatively high affinity between adsorbate and the adsorbent, also indicates chemisorption and the Langmuir isotherm model is suitable for single-layer adsorption onto a surface with a finite number of identical sites and uniform energies of adsorption [19]. The model is represented by Eq. (1) Is as follows

$$\frac{1}{Q_e}=\frac{1}{Q_{mac}KC_e}+\frac{1}{Q_{max}} \qquad \text{Eq. (1)}$$

Where Ce is the equilibrium concentration of the adsorbate (mg l^{-1}), Qe is the equilibrium absorption capacity of adsorbate (mg g^{-1}), Qmax and K are Langmuir characteristic constants, indicating maximum adsorption capacity (mg g^{-1}) and the energy of adsorption (L mg-1), respectively. The Freundlich-type model is used when the adsorption process is assumed to take place on a heterogeneous surface that varies with surface coverage [20]. The Freundlich isotherm is represented by Eq. (2)

$$\ln Qe = \ln k + (1/n) \ln Ce \qquad \text{Eq. (2)}$$

Where k and 1/n are the Freundlich characteristic constants, which indicate the adsorption capacity and adsorption intensity. Ce and Qe in Eq. (1) are the same as in Eq. (2). The isotherm data of fluoride and chromium adsorption on the rGO/Calcium alginate beads in water are shown in Fig. 8 the plots of Ce/Qe versus Ce and log Qe versus Log Ce for fluoride are given in Fig. 8 a and b while that of for chromium the plot of Ce/Qe versus Ce and log Qe versus log Ce are shown in Fig. 8 c and d. The fluoride and chromium adsorption constants and R^2 calculated using the two models are also listed in Table 1. According to the coefficient of determination (R^2), it is shown that the Langmuir model describes fluoride and chromium adsorption on the rGO-Calcium alginate beads better than the Freundlich model. Also, the Langmuir model is best fitted for fluoride adsorption as compared to chromium adsorption. So it shows monolayer adsorption. In addition, a dimensionless constant called separation factor, R_L, can be used to express an essential feature of Langmuir isotherm

$$R_L=\frac{1}{1+aC_m} \qquad \text{Eq. (3)}$$

Where C_m is the initial concentration (20 mg/L, in this case) of fluoride. The value of R_L indicates the type of the isotherm to be either unfavourable when $R_L>1$, linear if $R_L=1$, and favourable if $0<R_L< 1$ or $R_L=1$. The calculated R_L value for fluoride is 0.045 while for chromium the R_L value is 0.1359 indicating that the adsorption of the fluoride and chromium was a favorable process.

ISSN PRINT 2319 1775 Online 2320 7876
 Journal Volume 11 S Iss 01, 2022

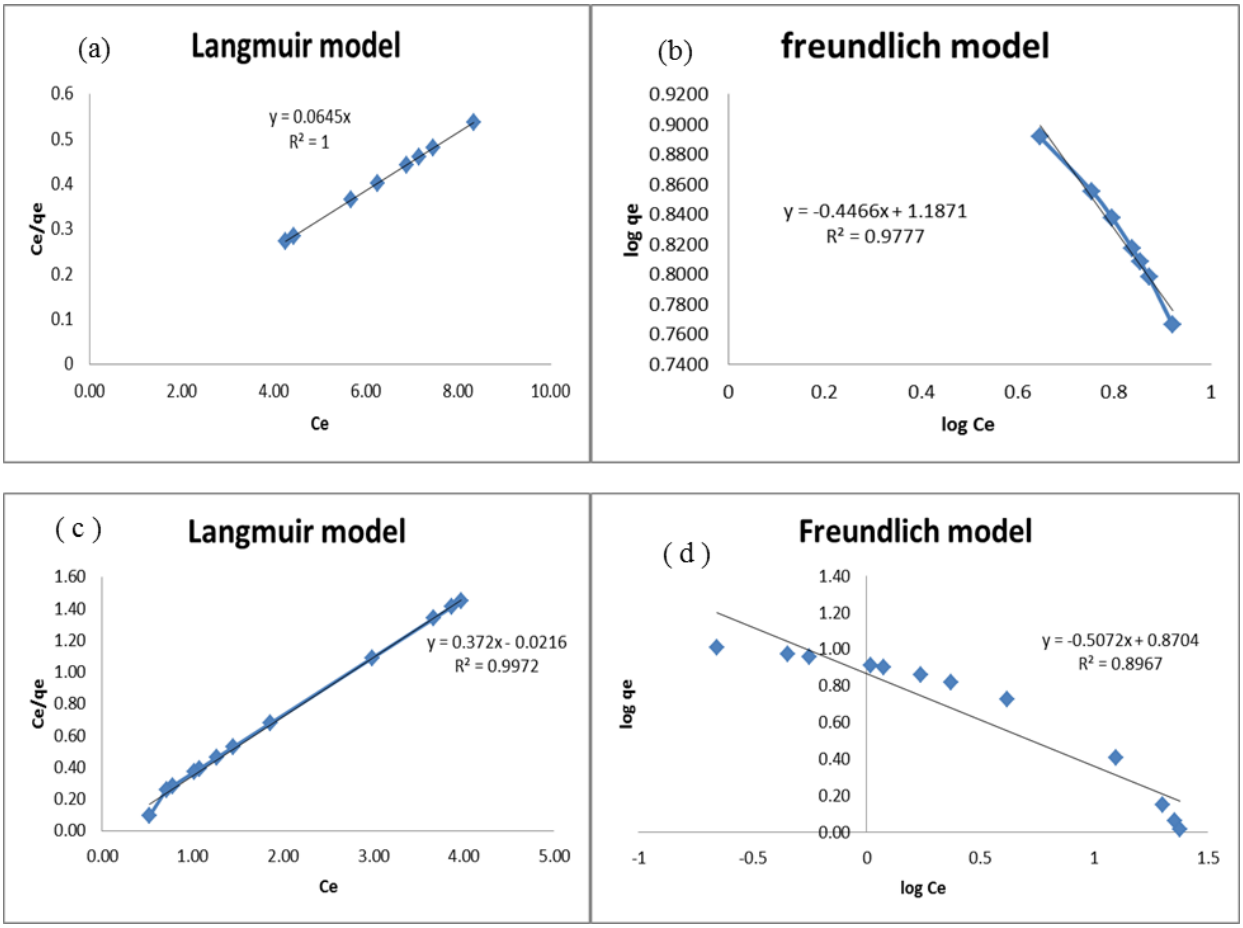

Fig.8 (a) Langmuir isotherm plot for fluoride removal (b) Freundlich isotherm plot for fluoride removal (c) Langmuir isotherm plot for chromium removal (d) Freundlich isotherm plot for chromium removal

Table 1 Langmuir isotherm, Freundlich isotherm data for fluoride and chromium removal

Langmuir isotherm for fluoride removal					**Frueundlich isotherm for fluoride removal**			
Temp.	Qmax	B	RL	R	Temp.	kF	1/n	R
273 k	15.50	0.0292	0.2551	1	273	3.2775	0.4466	0.9777

Langmuir isotherm for chromium removal					**Fruendlich isotherm for chromium removal**			
Temp.	Qmax	B	RL	R	Temp	kF	1/n	R
273	2.688	0.168	0.056	0.9972	273	2.3878	0.5072	0.8967

The pseudo-first and second-order kinetic models were tested for the removal of fluoride and chromium. Pseudo-first-order and pseudo-second-order model for fluoride removal is shown in Fig.9 (a) and (b) while pseudo-first-order and pseudo-second-order for chromium removal are shown in Fig. 10. (a) and (b) respectively. The pseudo-first-order model was plotted against

ISSN PRINT 2319 1775 Online 2320 7876
 Journal Volume 11 S Iss 01, 2022

log (q_e-q_t) versus time (t) and the pseudo-second-order kinetics model was plotted against t/q_t versus time (t). The kinetics study of adsorption provides information about the adsorption mechanism, as it shows the efficiency of the adsorption process. The values of K_1, K_2 and are given in Table 2 for fluoride and Table 3 for chromium removal. The values of the regression coefficient in chromium removal for pseudo-first and second-order rate equations are 0.955 and 0.991, respectively. While in chromium removal the R^2 for pseudo first and second-order rate equations are 0.966 and 0.979. From the R^2 values, it can be seen that the adsorption of fluoride and chromium ions from aqueous solutions is best described by the pseudo-second-order Lagergreen equation. This model is based on the assumption that the fluoride and chromium sorption process follows second-order chemisorption.

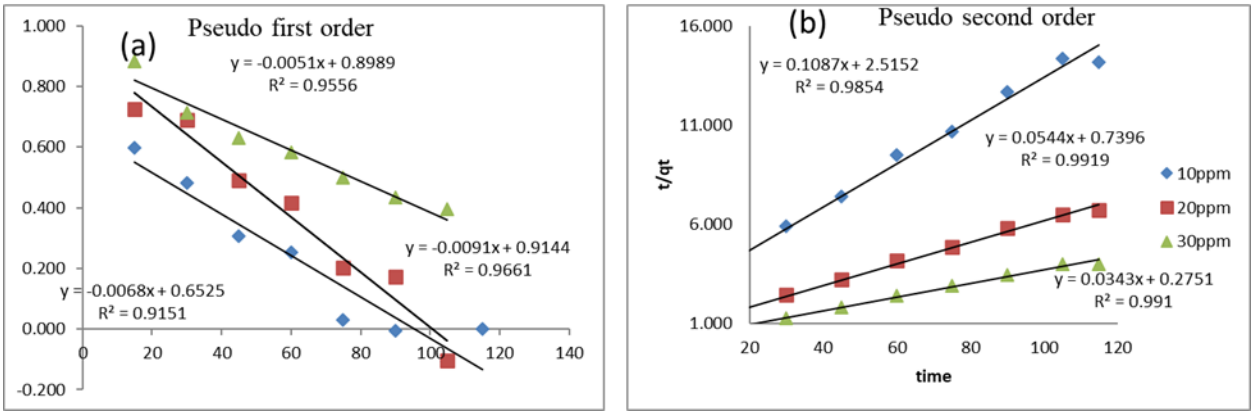

Fig. 9 (a) Pseudo-first order model. (b) Pseudo second order model for fluoride removal.

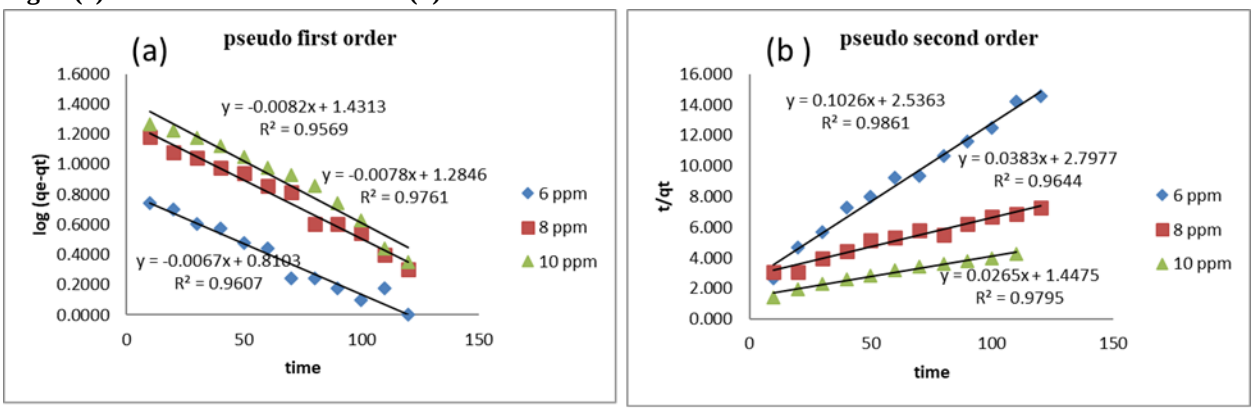

Fig. 10 (a) Pseudo-first order model. (b) Pseudo second-order model for chromium

Table 2 Adsorption kinetics constants of fluoride removal by rGO/calcium alginate obtained from pseudo first and second-order kinetics at different initial concentrations

	Pseudo first order			**Pseudo second order**		
Concentration	K_1	qe	R^2	K_2	qe	R^2
10 ppm	0.0138	1.5337	0.915	0.2487	0.3976	0.985
20 ppm	0.0207	1.0940	0.966	0.1243	1.3531	0.991
30 ppm	0.0115	1.1135	0.955	0.0783	3.6363	0.991

Table 3 Adsorption kinetics constants of chromium removal by rGO/calcium alginate obtained from pseudo-first and second-order kinetics at different initial concentrations

	Pseudo first order			Pseudo second order		
concentration	K_1	Qe	R^2	K_2	Qe	R^2
6 ppm	0.01381	1.2345	0.960	0.2349	0.3943	0.986
8 ppm	0.1612	0.7788	0.976	0.0875	0.3575	0.964
10 ppm	0.0207	0.6653	0.966	0.0598	0.6910	0.979

A plot of adsorbate uptake versus the square root of time would give a linear relationship if the intraparticle diffusion obeys the sorption process and if this line passes through the origin, then the particle diffusion would be the rate-controlling step. From the Fig. 11, it is clear that the plots are linear but do not pass through the origin. It indicates that intraparticle diffusion is involved in the adsorption but it is not the rate controlling step. This confirms that the removal of fluoride and chromium involves other mechanisms involving adsorption on the external surface and diffusion into the internal sites. In the following Table 4, the intraparticle diffusion rate constants k_{id} and the intercepts (I) obtained from the plots are shown. The intercepts of the plots indicate the boundary layer thickness. The larger the value of the intercept greater the contribution of the surface adsorption. From Table 4, it seems that with an increase in initial dye concentration, the values of intercepts also increase, indicating that the boundary layer effect increases with an increase in concentration.

ISSN PRINT 2319 1775 Online 2320 7876
 Journal Volume 11 S Iss 01, 2022

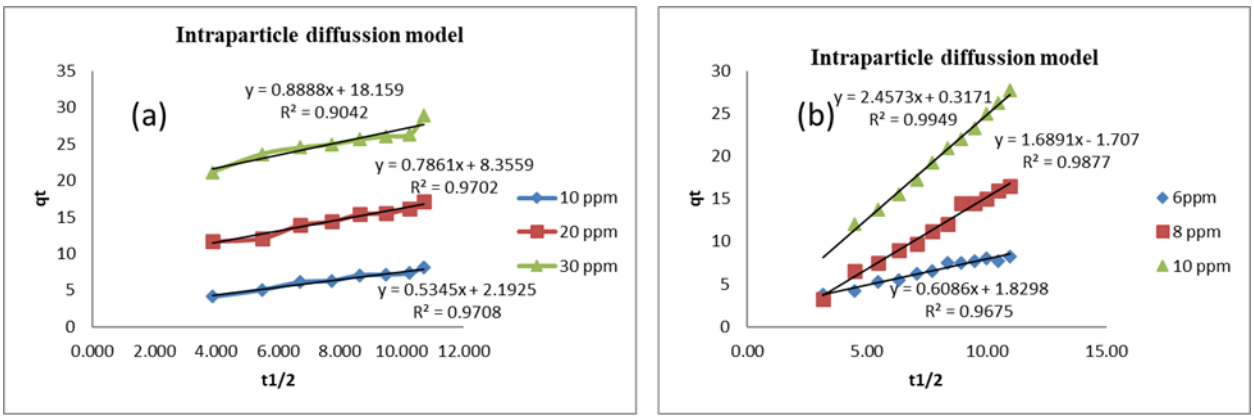

Fig.11 Intra particle diffusion model of (a) fluoride removal and (b) chromium removal by using r GO/calcium alginate beads.

Table 4: Intra particle diffusion constants and intercepts for fluoride and chromium removal by rGO/calcium alginate beads

Concentration For fluoride removal	K_{id} intraparticle diffusion constant	Intercept (I)	Correlation coefficient (R^2)
10ppm	1.2298	2.191	0.970
20ppm	1.8101	8.355	0.970
30 ppm	2.0450	18.15	0.904

4. Conclusion:

In summary, the removal of fluoride and chromium ions by using rGO/calcium alginate bead was studied. The adsorption isotherm data was fitted by Langmuir isotherms and the maximum adsorption capacity of the rGO/calcium alginate beads for fluoride removal and chromium removal was found to be 8.69 mg g^{-1} and 2.68 mg g^{-1}, respectively. The adsorption kinetics data were described by a pseudo-second-order kinetic equation.

References:

1. Y. Wang, Y. Qi, Y. Li, J. Wu, X. Ma, C. Yu, L. Ji, J. Hazard. Mater. 260, 9–15 (2013).
2. V.B.H. Dang, H.D. Doan, T. Dang-Vu, A. Lohi, Bioresour. Technol. 100, 211–219 (2009).
3. M. Baunthiyal, S. Ranghar, CLEAN Soil Air Water 43, 127–132 (2015).
4. 4. X.H. Guan, J.S. Du, X.G. Meng, Y.K. Sun, B. Sun, Q.H. Hu, (vol 215, pg 1, 2012). J. Hazard. Mater. 221(2012), 303 (2012)
5. Mahramanlioglu, M., Kizilcikli, I., Bicer, I.O., J. Fluorine Chem.,115 (1), 4147 (2002).
6. Ayoob, S., Gupta, A.K., Crit. Rev. Environ. Sci. Technol., 36, 433487 (2006).

7. A.A.M Daifullah, Yakout, S.M., Elreefy, S.A., J. Hazard. Mater. 147 (1/2), 633-643 (2007).
8. Shihabudheen, M.M., Atul, K.S., Ligy, P., Water Res., 40 (19), 3497-3506(2006).
9. Aldaco, R., Garea, A., Irabien, A., Water Res., 41 (4), 810-818 (2007).
10. Akbar, E., Maurice, S.O., Aoyi, O., Shigeo, A., J. Hazard. Mater, 152 (2), 571579 (2008).
11. Meenakshi, S., Viswanathan, N., "Identification of selective ion-exchange resin for fluoride sorption", J. Colloid Interface Sci., 308 (2), 438450 (2007).
12. Tor, A., "Removal of fluoride from water using anion-exchange membrane under Donnan dialysis condition", J. Hazard.Mater.,141 (3), 814818 (2007).
13. Lahnid, S., Tahaikt, M., Elaroui, K., Elmidaoui, A., "Economic evaluation of fluoride removal by electrodialysis", Desalination,230 (1/3), 213219 (2008).
14. Sehn, P.Desalination,223 (1/3), 7384 (2008).
15. Liu, J, Xu, Z., Li, X., Zhang, Y., Zhou, Y., Wang, Z., Wang, X., Sep. Purif. Technol.,58 (1), 5360 (2007).
16. Chauhan, V.S., Dwivedi, P.K., Iyengar, L., J. Hazard. Mater., 139 (1), 103107 (2007).
17. Ayoob, S., Gupta, A.K., J. Hazard. Mater., 152 (3), 976985 (2008).
18. Ghorai, S., Pant, K.K., Sep. Purif. Technol.,42 (3), 265271 (2005).
19. Mohapatra, D., Mishra, D., Mishra, S.P., Roy Chaudhury, G., Das, R.P., J. Colloid Interface Sci.,275 (2), 355359 (2004).
20. Sarkar, M., Banerjee, A., Pramanick, P.P., Sarkar, A.R., J.Colloid InterfaceSci.,302 (2), 432441 (2006).
21. Tor, A., Desalination,201 (1/3), 267276 (2006).
22. Coetzeel, P.P., Coetzee, L.L., Pukal, R., Mubenga, S., "Characterisation of selected South African clays for defluoridation of natural waters", Water SA.,29 (3), 331338 (2003).
23. Fan, X., Parker, D.J., Smith, M.D., Water Res.,37 (20), 49294937 (2003).
24. Ramos, R.L., Ovalle-Turrubiartes, J., Sanchez-Castillo, M.A., Carbon, 37 (4), 609617 (1999).
25. M.S. Onyango, Y. Kojima, O. Aoyi, E.C.Bernardo, H. Matsuda,Chin. J.Colloid Interface Sci., 279 (2), 341350 (2004).
26. Chidambaram, S., Ramanathan, A.L., Vasudevan, S., Water SA., 29 (3), 339344 (2003).
27. Wu, H.X., Wang, T.J., Chen, L., Jin, Y., Ind.Eng.Chem.Res.,48 (9), 45304534 (2009).
28. S. K. Singh, S. Lawrance, J. Bajpai and A. K. Bajpai, Int. J. Eng. Res. & Technol., vol. 2, pp. 1-11, Oct. 2013.
29. M.G. Sujana, A.Mishra, and B.C. Acharya, Appl. Surf. Sci., vol. 270, pp. 767–776, April 2013.
30. S. M. Prabhu and S. Meenakshi, Carbohydr. Polym., vol. 120, pp. 60–68, Dec. 2015.
31. K. Pandi and N. Viswanathan, J. Appl. Polym. Sci., pp. 1-9, May 2015.
32. R. kumar, S.J. Kim ,K.S. Kim, S.H. Lee, H.S park, B.H.Jeon

ISSN PRINT 2319 1775 Online 2320 7876
 Journal Volume 11 S Iss 01, 2022

33. M. R. Hoffmann, S. T. Martin, W. Y. Choi, D. W. Bahnemannt. Chem. Rev. 95 (**1995)** 69.
34. L.B.Li,Y.P.Fang, R.Vreeker, I.Appelqvist. Biomacromolecules 8 **(2007)** 464.
35. S.K.Papageorgiou, E.P.Kouvelos, E.P. Favvas, A.A. Sapalidis, G.E. Romanos, F.K. Katsaros. Carbohydr Res 345 **(2010)** 469.
36. Langmuir. J. Am. Chem. Soc. 38 **(1916)** 2221.
37. H. Freundlich. Z. Phys. Chem-Stoch. 57 **(1906)** 385.
38. J.N. Tiwari, K. Mahesh, N.H. Le, K.C. Kemp, R. Timilsina, R.N.Tiwari, K.S. Kim. Carbon 56 **(2013)** 173.
39. M. Baunthiyal, S. Ranghar. CLEAN Soil Air Water 43 **(2015)** 127.

ISSN PRINT 2319 1775 Online 2320 7876
 Journal Volume 11 S Iss 01, 2022